https://doi.org/10.31891/2219-9365-2026-87-34
UDC 621.396:004.62

DRUZHYNIN Volodymyr
Taras Shevchenko National University of Kyiv
https://orcid.org/0000-0002-5340-6237
e-mail: volodymyr.druzhynin@knu.ua
BONDARENKO Olha
Taras Shevchenko National University of Kyiv
https://orcid.org/0000-0003-0024-8789
e-mail: olha.bondarenko@knu.ua

TIME SYNCHRONIZATION THRESHOLDS FOR FUSION LEVELS IN MULTISENSOR RADIO MONITORING

The paper analyses how time synchronization accuracy between sensor nodes affects the probability of erroneous decision in a multisensor radio monitoring system. The fusion level of sensor streams (primary observations, features, or local decisions) is shown to be a structural parameter that determines which time scale governs the tolerable synchronization error.

A two-sensor model of distributed reception with independent Gaussian timing offsets is constructed. For each of the three fusion levels, the dependence of the probability of error on the synchronization-error standard deviation is derived analytically; the primary-level expression is obtained as an expectation over the Gaussian phase-jitter distribution. It is shown that at the local-decision and feature levels the relevant time scale is the symbol duration or the integration window, while at the primary level it becomes the carrier period, which is several orders of magnitude shorter at radio frequencies.

The derived primary-level expression is verified by Monte Carlo simulation of the same two-sensor signal model under Gaussian phase jitter. The analytical dependence and the simulation results agree across the full range of synchronization-error values. The simulation is repeated for three values of the per-sensor signal-to-noise ratio (0, 5, 10 dB) and for three representative carrier frequencies (100 MHz, 433 MHz, 2.4 GHz), confirming that the location of the transition region is independent of the signal-to-noise ratio and scales as 1/(2π · fc) with the carrier frequency.

The accuracy regimes of established time-distribution standards (NTP, IEEE 1588 PTP in software and hardware variants, GNSS-disciplined oscillators, White Rabbit) are qualitatively mapped onto the fusion levels for which these standards may be applicable, with the actual limit depending on the carrier frequency. The results enable joint selection of synchronization accuracy and fusion algorithm at the design stage of a multisensor system.

Keywords: multisensor systems, radio monitoring, time synchronization, fusion level, IEEE 1588, White Rabbit, probability of error, primary-level fusion, Monte Carlo simulation.

ДРУЖИНІН Володимир, БОНДАРЕНКО Ольга
Київський національний університет імені Тараса Шевченка

ПОРОГИ ТОЧНОСТІ ЧАСОВОЇ СИНХРОНІЗАЦІЇ ДЛЯ РІЗНИХ РІВНІВ ІНТЕГРАЦІЇ В МУЛЬТИСЕНСОРНИХ СИСТЕМАХ РАДІОМОНІТОРИНГУ

У статті досліджено, яким чином точність часової синхронізації між сенсорними вузлами впливає на ймовірність прийняття хибного рішення у мультисенсорній системі радіомоніторингу. Обґрунтовано, що рівень інтеграції сенсорних потоків є структурним параметром системи, який визначає часовий масштаб, що обмежує допустиму похибку синхронізації: на рівнях локальних рішень та ознак цим масштабом є тривалість символу або інтеграційного вікна, а на рівні первинних спостережень – період несучої частоти, який на радіочастотах коротший на кілька порядків.

Для двосенсорної BPSK-моделі первинної когерентної інтеграції аналітично виведено залежність ймовірності помилки від середньоквадратичного відхилення похибки синхронізації та підтверджено її моделюванням Монте-Карло. Точнісні режими наявних стандартів розподілу часу (NTP, IEEE 1588 PTP, GNSS-дисципліновані генератори, White Rabbit) орієнтовно зіставлено з рівнями інтеграції, для яких вони придатні. Отримані результати дозволяють вибирати точність синхронізації разом із алгоритмом інтеграції на етапі проєктування мультисенсорної системи.

Ключові слова: мультисенсорні системи, радіомоніторинг, часова синхронізація, рівень інтеграції, IEEE 1588, White Rabbit, ймовірність помилки, інтеграція первинних даних, моделювання Монте-Карло.

Стаття надійшла до редакції / Received 07.06.2026
Прийнята до друку / Accepted 27.08.2026
Опубліковано / Published 10.09.2026

STATEMENT OF THE PROBLEM

Distributed multisensor architectures are widely used in modern radio monitoring systems. Such systems address the challenges of spectrum management, emission source detection, and electromagnetic environment assessment. The spatial separation of sensor nodes allows for the coverage of large geographic areas, the localization of emission sources using triangulation, and the maintenance of operational capability in the presence of local interference. Implementing these capabilities requires aligning local time scales: each sensor operates on its own local time scale, so to combine observations from different sensors into a consistent description of a physical phenomenon, these scales must be aligned with sufficient precision.

The timing mechanism in practical systems is selected based on cost, network topology, and available infrastructure, and is not typically considered a parameter of the detection problem itself. It is commonly assumed that if the absolute synchronization error is small, its contribution to the quality metrics of the decision is also small. This assumption holds true for quantities that are insensitive to small time shifts (e.g., local binary decisions) and ceases to hold when time alignment is embedded in the signal itself.

In the author's previous work, it was demonstrated that the sensor information fusion level is a structural parameter of a multisensor radio monitoring system that directly affects the achievable lower bound on the probability of an erroneous decision. This article shows that the same parameter also determines the system's sensitivity to synchronization errors: the same synchronization error leads to qualitatively different consequences depending on the chosen fusion level. When transitioning from the fusion of local decisions or features to the fusion of primary observations, the characteristic time scale is reduced by several orders of magnitude.

The aim of this study is to determine how the accuracy of time synchronization between sensor nodes affects the probability of making an erroneous decision in a multisensor radio monitoring system, and how the nature of this effect depends on the chosen fusion level.

Within the scope of the stated objective, the following tasks are addressed:

1. to construct a model of the observation time error in a two-sensor radio monitoring system and show how the synchronization contribution depends on the fusion level;
2. to describe the difference in time scales for the fusion of local decisions, features, and primary observations, and show that for primary I/Q data, phase jitter at the carrier frequency becomes the determining factor;
3. to derive the relationship between the probability of an erroneous decision and the root mean square (RMS) error of synchronization for a basic two-sensor BPSK model of primary coherent integration;
4. to verify the derived expression for the level of primary observations using Monte Carlo simulation;
5. to investigate, through simulation, the effect of the signal-to-noise ratio and carrier frequency on the location of the transition region where the error probability degrades;
6. to provide an engineering interpretation of the obtained dependencies and roughly correlate typical synchronization modes with the fusion levels for which they may be suitable.

THEORETICAL BACKGROUND AND RELATED WORKS

Statistical and Architectural Foundations of Distributed Detection. The classical framework for fusing decisions from spatially dispersed sensors is presented in [1-3] and remains the basis for analyzing how local decision-making rules are integrated into a global one. Within this framework, observations are considered temporally synchronized, and the effects of imperfect synchronization are accounted for by a general noise component with fixed variance. References [4, 5] extend this scheme to wireless sensor networks, taking into account channel fading and imperfections, and refine the channel model; however, the assumption of time synchronization at the fusion center remains unchanged. The information-theoretic upper bound on the achievable error probability for any preprocessing transformation follows from the data processing inequality and the Fano inequality [6]; however, this bound does not provide a direct dependence on synchronization accuracy.

Time-triggered architectures for sensor data fusion. The approach that treats time as an architectural parameter of the system rather than an implementation issue originates from the work [7] on distributed real-time systems with time triggers. This approach has been applied to sensor data fusion in [8]. Confidence-weighted averaging between nodes requires a common global time scale for all participants, making synchronization at the architectural level a factor that influences the set of possible fusion strategies. In this context, the corresponding analysis was performed for the automotive and aviation industries, where the primary accuracy requirement is in the microsecond range, and the carrier frequency sensitivity characteristic of radio-frequency systems does not arise.

Synchronization Standards and Their Accuracy Modes. The primary standard for network time distribution is the IEEE 1588 Precision Time Protocol [9]. On standard Ethernet, the typical achievable accuracy is a few microseconds, while implementations with hardware support reach the sub-microsecond range. The High-Accuracy profile, included in IEEE 1588-2019, is based on the White Rabbit extension developed at CERN. This extension uses synchronous Ethernet for synchronization and a calibrated line-delay model, enabling sub-nanosecond accuracy with picosecond precision [10]. An alternative reference is GNSS-disciplined oscillators, which are tied to UTC with an uncertainty of tens of nanoseconds [11]. The NTP protocol provides accuracy ranging from milliseconds on local networks to tens of milliseconds over the public Internet [12].

Synchronization in radio monitoring tasks. Applied research on distributed radio-frequency sensing, including studies of cognitive MANET radio networks [13], the detection of emission sources using UAVs [14], and infrastructure recommendations from international organizations [15, 16], considers synchronization to be one of the technical prerequisites. In practical implementations, it is specified via a chosen standard (PTP, GNSS-disciplined oscillators) rather than derived from the required detection quality metrics. The inverse problem (namely, determining the synchronization mode given a specified target error probability and fusion level) has not been formalized in the literature on distributed radio monitoring.

The analyzed literature therefore reveals four partially disconnected research directions:

1. in algorithmic theory, decision-making rules are optimized under the assumption of fixed time alignment;
2. in time-triggered architectures, the need for a common time scale is justified, but the analysis does not extend to radio-frequency carriers;
3. in synchronization standards, accuracy is characterized in absolute time units without linking it to detection quality;
4. in applied radio monitoring research, synchronization is treated primarily as an implementation requirement rather than as a parameter of the decision-making model.

This article bridges the gap between these directions. It derives the dependence of the error probability on synchronization accuracy as a function of the fusion level, and the resulting expression is verified by Monte Carlo simulation for a two-sensor model.

PRESENTATION OF THE MAIN MATERIAL

A Model of Synchronization Error in Distributed Radio Monitoring

The subject of analysis is a multisensor radio monitoring system with two spatially separated nodes that observe a common electromagnetic phenomenon. This phenomenon is described by the hypotheses H_0 (signal absent) and H_1 (signal present). Each sensor $i \in \{1,2\}$ generates an observation

$$y_i(t) = g_i(s(t-\Delta t_i)) + \varepsilon_i(t), \tag{1}$$

where $s(t)$ is the useful signal, $g_i(\cdot)$ is the reception and preprocessing operator of the *i*-th sensor, $\varepsilon_i(t)$ is local additive noise, and Δt_i is the offset between the local time scale of the *i*-th sensor and the system's nominal time scale.

Synchronization offsets are modeled as independent Gaussian random variables with a mean of zero

$$\Delta t_i \sim \mathrm{N}\ (0, \sigma_{\Delta t}^2), \tag{2}$$

where $\sigma_{\Delta t}$ denotes the root mean square deviation of the relative synchronization error between sensor nodes and characterizes the residual jitter of the time distribution infrastructure after applying the selected synchronization protocol. It is this quantity that is operationally significant, since the specified characteristics of time distribution standards (NTP, IEEE 1588 PTP, GNSS-disciplined oscillators, White Rabbit) pertain to relative accuracy between nodes, rather than absolute offsets relative to a reference standard. Values $\sigma_{\Delta t}$ range from approximately 10^{-3} s for NTP on the open Internet to approximately 10^{-10} s for White Rabbit installations [9, 10, 12].

We can express the total variance of the joint distribution of observations as follows:

$$\sigma_{total}^2 = \sigma_{obs}^2 + \sigma_{sync}^2(\sigma_{\Delta t}, \lambda), \tag{3}$$

where σ_{obs}^2 is the variance of receiver noise and channel effects, $\sigma_{sync}^2(\sigma_{\Delta t}, \lambda)$ is the variance component caused by synchronization error. The notation $\lambda \in$ {decision, feature, primary} indicates that the form σ_{sync}^2 depends on the chosen fusion level. The same root mean square error $\sigma_{\Delta t}$ results in qualitatively different contributions to the variance depending on which quantity is aggregated.

Probability of error at the three fusion levels

The three main fusion levels (local decisions, features, and primary data) differ in terms of which quantity the sensor transmits to the fusion center, as well as how the bias Δt_i affects the aggregated observation.

Local-decision-level fusion. Each sensor performs its own detection and transmits a hard decision $d_i \in \{0, 1\}$. The fusion center combines the local decisions according to a specified fusion rule (logical "AND", logical "OR" or a weighted majority rule when there are at least three sensors). In this case, the synchronization error affects the result only through the position of the integration window in which the local decision is formed. If $|\Delta t_i|$ is small compared to the symbol duration T_{sym}, the local detector receives nearly the same signal as it would under ideal synchronization, so the local probability of error deteriorates only slightly. The signal-to-noise ratio loss coefficient per sensor is expressed as

$$SNR_{eff} = SNR \cdot D_{dec}\left(\frac{\sigma_{\Delta t}}{T_{sym}}\right), \tag{4}$$

where $D_{dec}(\cdot)$ is a degradation function that is close to one when $\sigma_{\Delta t} << T_{sym}$ and decreases to zero as $\sigma_{\Delta t}$ approaches T_{sym}. The dependence is determined by the ratio of the root mean square (RMS) synchronization error to the symbol duration, i.e., the baseband time scale.

Feature-level fusion. Each sensor calculates a feature (typically the signal energy within a specified window, a bin value from a spectrogram, or a similar statistic) and transmits it to the fusion center, which combines the features and then makes a decision. Synchronization errors shift the integration windows of different sensors relative to one another, causing some of the energy that should have fallen within the window to be lost. For a window of duration $T_W >> T_{sym}$ and under the condition $\Delta t_i \sim \mathrm{N}\ (0, \sigma_{\Delta t}^2)$ the average energy retention coefficient is expressed as

$$R_{feat}(\sigma_{\Delta t}) = E\left[\left(1 - \frac{|\Delta t_i|}{T_W}\right)_+^2\right], \tag{5}$$

where $(\cdot)_+$ denotes the positive part. The effective signal-to-noise ratio at the fusion center is:

$$SNR_{eff} = N_s \cdot SNR \cdot R_{feat}(\sigma_{\Delta t}), \tag{6}$$

where N_s is the number of sensors. The factor $R_{feat}(\sigma_{\Delta t})$ is close to one when $\sigma_{\Delta t} << T_W$ and decreases gradually as $\sigma_{\Delta t}$ increases. The integration window T_W remains the dominant time scale here as well.

Primary-level fusion. Each sensor transmits its own primary I/Q samples to the fusion center, which are then coherently summed before any nonlinear processing or feature extraction. The offset Δt_i is converted into a phase shift of the received complex envelope at the carrier frequency f_c:

$$y_i(t) \to y_i(t - \Delta t_i) \approx s(t) \cdot \exp\left(j \cdot 2\pi \cdot f_c \cdot \Delta t_i\right) + \varepsilon_i(t). \tag{7}$$

The phase error $\varphi_i = 2\pi f_c \Delta t_i$ has a variance

$$\sigma_\varphi^2 = (2\pi \cdot f_c)^2 \cdot \sigma_{\Delta t}^2. \tag{8}$$

Therefore, even nanosecond-scale time offsets generate phase errors of the order of one at UHF frequencies. The expected coefficient of coherent summation under a Gaussian phase distribution is given by the characteristic function

$$\rho(\sigma_{\Delta t}, f_c) = E\left[\exp\left(j \cdot 2\pi \cdot f_c \cdot \Delta t_i\right)\right] = \exp\left(-2\pi^2 \cdot f_c^2 \cdot \sigma_{\Delta t}^2\right). \tag{9}$$

This coefficient varies from one in the case of ideal synchronization to zero in the case of complete decoherence.

A two-sensor model for BPSK detection in the presence of phase jitter. To express P_{err} in a form suitable for direct modeling, let us consider two coherent sensors that receive a BPSK-modulated signal. The sensor outputs are described by the equations:

$$x_1 = a \cdot b + n_1, \qquad x_2 = a \cdot b \cdot \exp(j \cdot \varphi) + n_2, \tag{10}$$

where a is the signal amplitude, $b \in \{-1, +1\}$ is the transmitted symbol, n_1, n_2 are independent complex Gaussian noise samples, and φ is the phase shift between the two sensors caused by synchronization error.

The coherent sum at the fusion center:

$$x = x_1 + x_2 . \tag{11}$$

The decision is made based on the real part x :

$$z = \mathrm{Re}\{x\} = a \cdot b \cdot (1 + \cos\varphi) + \eta , \tag{12}$$

where η is the residual real Gaussian noise.

By convention $SNR := a^2 / N_0$, where N_0 denotes the total complex noise power per sensor, the real part of each n_i is Gaussian with mean zero and variance $N_0 / 2$. After coherent summation in (11) and projection onto the real axis in (12), the decision noise η is Gaussian with a mean of zero and variance

$$\sigma_\eta^2 = \frac{N_0}{2} + \frac{N_0}{2} = N_0 = \frac{a^2}{\mathrm{SNR}} . \tag{13}$$

Therefore, the conditional probability of error given a specific φ is:

$$P_{err}(\varphi) = Q\left(\sqrt{\mathrm{SNR}} \cdot (1 + \cos\varphi)\right), \tag{14}$$

where $Q(\cdot)$ is the Gaussian Q- function. Averaging over the distribution φ yields the unconditional probability of error:

$$P_{err}(\sigma_{\Delta t}, f_c, \lambda = \text{primary}) = E_\varphi\left[Q\left(\sqrt{\mathrm{SNR}} \cdot (1 + \cos\varphi)\right)\right], \tag{15}$$

where

$$\varphi \sim \mathrm{N}\left(0, (2\pi \cdot f_c)^2 \cdot \sigma_{\Delta t}^2\right). \tag{16}$$

Equation (15) describes how the probability of error depends on the root mean square deviation of the synchronization error within the framework of the accepted two-sensor BPSK model. The determining time scale here is the carrier period T_c, which, for typical combinations of carriers and radio monitoring signal bands, is several orders of magnitude shorter than the symbol duration T_S. Degradation due to phase jitter begins when σ_φ becomes of the order of unity, i.e., when $\sigma_{\Delta t} = 1/(2\pi \cdot f_c)$. When transitioning from the level of local decisions or features to the level of primary data, the time scale that determines the permissible synchronization error changes abruptly. Within the framework of coherent integration of primary I/Q samples without additional estimation and compensation of phase shift, this time scale cannot be eliminated by choosing a fusion rule. A two-sensor BPSK model is used as a basic analytical scenario, allowing us to explicitly trace the transition of the time error into phase jitter and obtain a closed-form expression for the error probability. Generalization to other modulation schemes, the number of sensors, and fusion rules changes the specific form P_{err}, but does not eliminate the dependence of phase mismatch on the product $2\pi \cdot f_c \cdot \sigma_{\Delta t}$.

Numerical Verification of the Derived Expression Using Monte Carlo Simulation

The numerical accuracy of the resulting expression (15) was verified using Monte Carlo simulation based on the same two-sensor BPSK signal model (10)-(14) with phase shifts generated according to (16). For each value of

$\sigma_{\Delta t}$, 4×10^5 independent symbols were processed. The carrier frequency was set to f_c = 433 MHz, and the signal-to-noise ratio (SNR) at the sensor was 5 dB. The root mean square (RMS) deviation of the synchronization error varied from 10^{-12} s to 10^{-5} s according to a logarithmic distribution. The empirical error probability obtained from the simulation was compared with the value (15), calculated by numerical integration over a Gaussian distribution φ. The results are shown in Fig. 1.

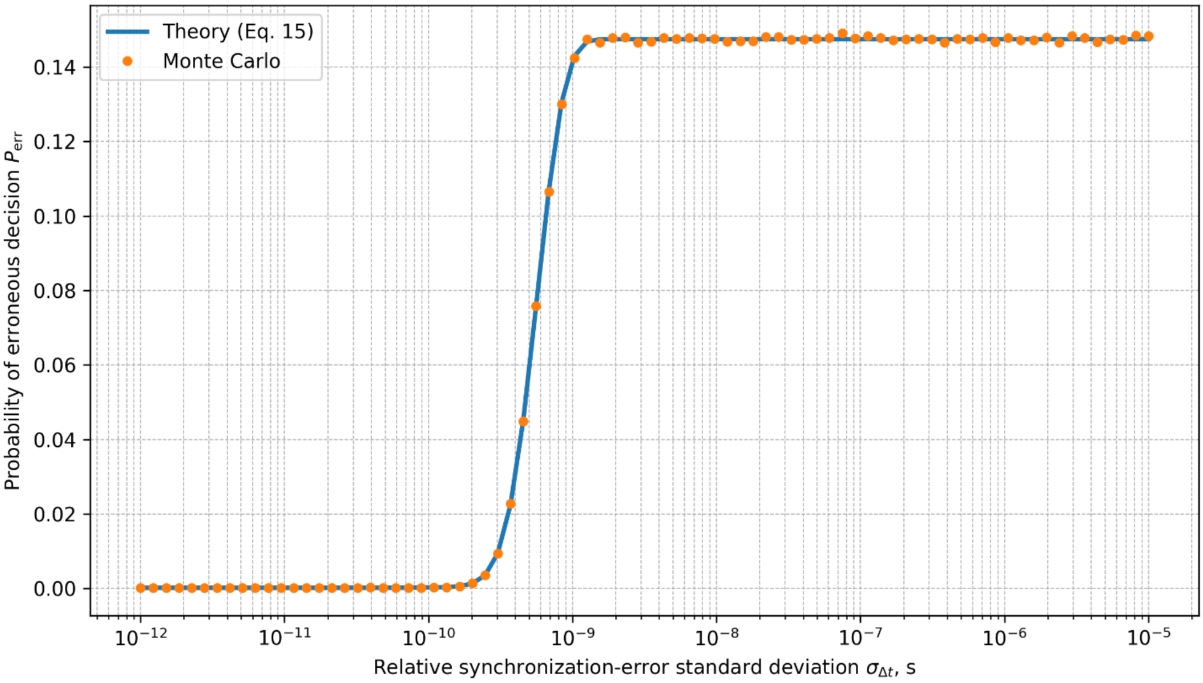

Fig. 1. Verification of the derived expression for the level of primary observations

The simulation reproduces the analytical curve over the entire range under study $\sigma_{\Delta t}$. The probability of error remains at a level limited by the SNR for $\sigma_{\Delta t}$ below 10^{-10} s. It then passes through a transitional region near $\sigma_{\Delta t} \approx 3.7\cdot10^{-10}$ s and converges to an asymptotic value for large jitter values. The discrepancies between the analytical and empirical values fall within the statistical error of the Monte Carlo estimate. This confirms that expression (15) correctly describes the model (10)-(14).

To investigate the effect of the signal-to-noise ratio on the obtained dependence, the simulation was repeated at f_c = 433 MHz for three values of SNR ∈ {0, 5, 10} dB. The results are shown in Fig. 2. Increasing the signal-to-noise ratio shifts the entire curve downward along the error probability axis, while the position of the transition region remains near $\sigma_{\Delta t} \approx 1/(2\pi \cdot f_c)$. This transition region, caused by phase jitter, is practically independent of the signal-to-noise ratio; therefore, improving the receiver's noise performance does not reduce the requirements for the synchronization infrastructure.

The dependence of the transition region's position on the carrier frequency is shown in Fig. 3. The simulation was performed at SNR = 5 dB for f_c ∈ {100 MHz, 433 MHz, 2.4 GHz}. As the carrier frequency increases by an order of magnitude, the transition region shifts by approximately one order of magnitude toward lower values of $\sigma_{\Delta t}$: degradation begins near 1.6 ns at 100 MHz, near 370 ps at 433 MHz, and near 66 ps at 2.4 GHz. This directly illustrates the scaling $\sigma_{\Delta t} \approx 1/(2\pi \cdot f_c)$ predicted by equations (8) and (9) and explains why coherent integration of primary data in the upper UHF and microwave bands requires sub-nanosecond or picosecond synchronization accuracy.

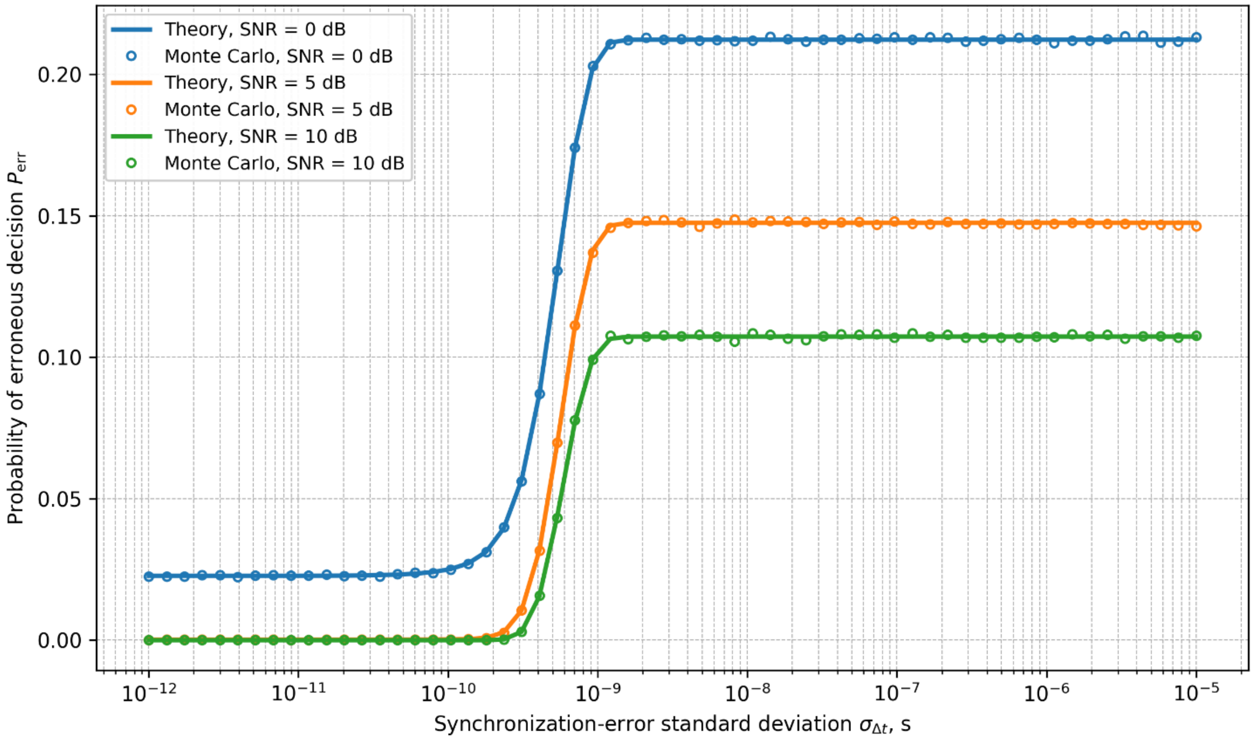

Fig. 2. Effect of the signal-to-noise ratio on the dependence $P_{err}(\sigma_{\Delta t})$ at f_c = 433 MHz

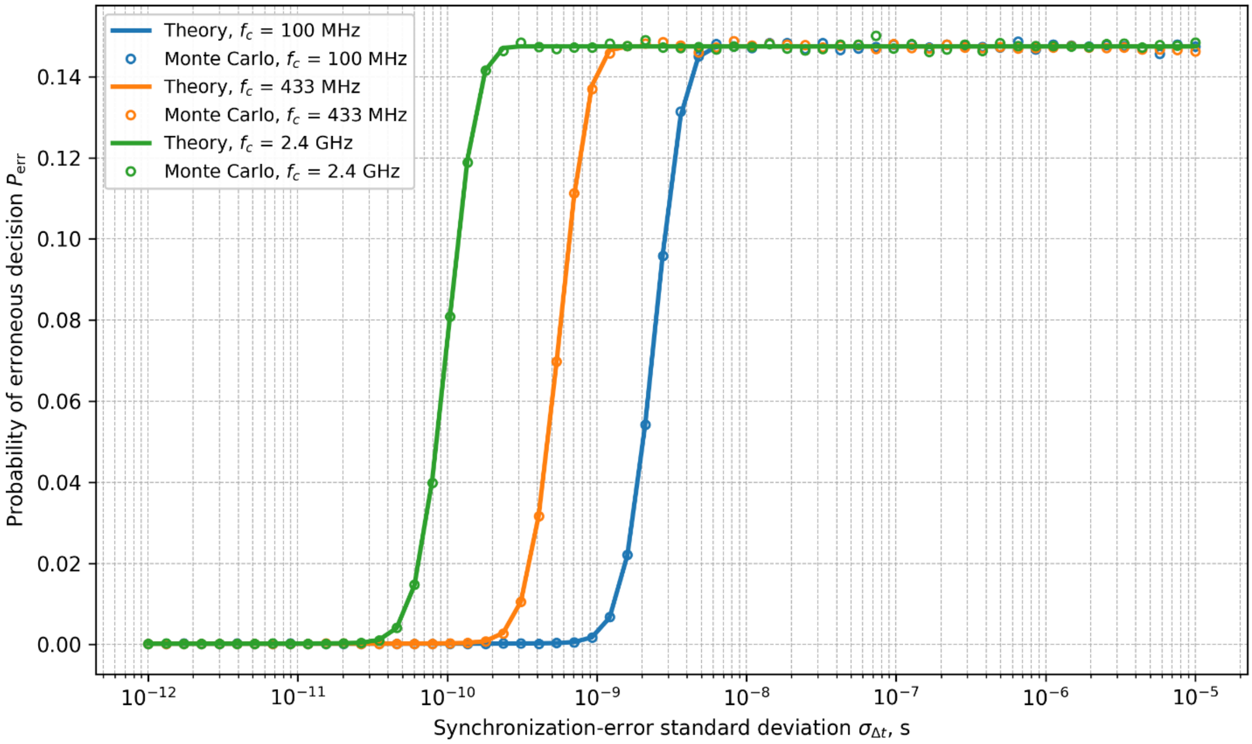

Fig. 3. Effect of the carrier frequency on the dependence $P_{err}(\sigma_{\Delta t})$ at SNR = 5 dB

Engineering Interpretation of Synchronization Requirements

The derived relationships allow us to evaluate the suitability of the synchronization mode for a given fusion level. For the primary observation level, phase jitter $2\pi \cdot f_c \cdot \sigma_{\Delta t}$ is the determining factor, so the permissible synchronization error depends directly on the carrier frequency. The exact threshold value $\sigma_{\Delta t}$ for given SNR, f_c and permissible level P_{err} can be found from Equation (15).

For feature and local decision levels, it is not the carrier period but the symbol duration or integration window that is the determining factor; therefore, the same synchronization mode may be sufficient for integrating features or decisions but insufficient for the coherent combination of primary I/Q samples. This means that the choice of synchronization standard must be made in conjunction with the choice of fusion level.

A rough comparison of typical synchronization modes with fusion levels is shown in Table 1. This is not a universal rule: specific thresholds depend on the SNR, modulation, actual residual jitter, and the acceptable error probability level. If the synchronization mode is fixed by external constraints, the available accuracy determines whether fusion at the primary data level is possible or whether only feature or decision levels are available; conversely, given a target P_{err} and a fixed carrier frequency, Equation (15) allows one to calculate the minimum required synchronization accuracy.

Table 1

Approximate comparison of synchronization standards with fusion levels (BPSK, AWGN)

Standard/Mode	**Typical $\sigma_{\Delta t}$**	**Recommended fusion mode**
NTP, implementation via the open Internet	[illegible] s	Not suitable for primary coherent integration on any radio frequency carrier. May be used only for decision levels or features over very large time windows
NTP, implementation on a local network	[illegible] s	Not suitable for primary coherent integration on any radio frequency carrier. Suitable for decision and feature levels over sufficiently large time windows
IEEE 1588 PTP, software implementation	[illegible] s	Suitable for decision and feature levels over moderate baseband time scales. Not suitable for primary coherent integration on radio frequency carriers
IEEE 1588 PTP, hardware implementation	[illegible] s	Suitable for decision and feature levels. For primary coherent integration – only at very low carrier frequencies or with additional phase compensation
GNSS-disciplined reference oscillator	[illegible] s	Suitable for decision and feature levels. For primary coherent integration – limited applicability in the lower part of the radio frequency range; the exact limit is determined by Equation (15)
White Rabbit (IEEE 1588 HA), standard implementation	[illegible] s	Suitable for decision and feature levels. Potentially suitable for primary coherent integration; the specific carrier frequency limit depends on the actual residual jitter and is calculated from Equation (15)
White Rabbit, precision implementation	[illegible] s	Suitable for decision and feature levels. Potentially suitable for primary coherent integration in higher radio frequency bands, provided that the actual residual jitter is controlled

Limitations of the Study

The analysis presented here is based on a number of model assumptions that define the limits of applicability of the obtained results. The signal model is limited to BPSK modulation in a channel with additive white Gaussian noise; generalizations to higher-order modulations and channels with fading are beyond the scope of this work. The fusion architecture includes coherent summation of two sensors at the primary data level, simple energy summation within a window at the feature level, and a generalized rule for combining local decisions at the decision level; alternative fusion rules, such as likelihood-based combination or trained aggregation rules, are not considered. The synchronization error model assumes uncorrelated Gaussian inter-node offsets with a zero mean, which corresponds to the residual jitter mode of existing time-distribution standards, but does not describe correlated drift, deterministic scale shift, or behavior in autonomous mode during reference source interruptions. Numerical verification was performed using the same signal model from which the analytical expression was derived; it confirms the mathematical consistency of the expression, rather than its agreement with the results of hardware measurements.

CONCLUSIONS

This article provides an analytical study of how the accuracy of time synchronization between sensor nodes affects the probability of making an erroneous decision in a multisensor radio monitoring system. An observation error model is constructed in which the residual temporal uncertainty after applying the selected synchronization protocol is represented as an independent Gaussian variable with a mean of zero. The total observation variance is decomposed into a receiver noise component and a synchronization-induced component, the form of which explicitly depends on the fusion level.

It has been established that, at the levels of local decisions and features, the time scale that determines the permissible synchronization error coincides with the symbol duration or the integration window duration – that is, baseband quantities. At the level of primary data, this scale is the carrier period, which at radio frequencies is several orders of magnitude shorter. The transition between these modes is qualitative, and within the framework of coherent integration, it is impossible to eliminate it by selecting a fusion rule without additional estimation of the phase shift. For a two-sensor BPSK model, the dependence of the error probability on the root mean square deviation of the synchronization error is derived as the mathematical expectation under a Gaussian distribution of phase jitter (15).

The derived expression has been numerically verified using Monte Carlo simulations of the same signal model. The analytical expression and the empirical estimate agree closely over the entire range of synchronization error values; the simulation reproduces the transition near the carrier period time scale and the asymptotic behavior for large jitter values. Additional Monte Carlo experiments for three SNR values (0, 5, 10 dB) at f_c = 433 MHz and for three characteristic carrier frequencies (100 MHz, 433 MHz, 2.4 GHz) at SNR = 5 dB confirmed that the position of the transition region is practically independent of SNR and scales proportionally to $1/(2\pi \cdot f_c)$ as the carrier frequency increases.

A comparison with known synchronization standards showed that, for decision-level and feature-level architectures, hardware-based IEEE 1588 PTP and GNSS-disciplined oscillators provide sufficient accuracy in many practical scenarios. Fusion at the primary observation level imposes significantly stricter requirements, which must be evaluated separately for a specific carrier frequency, the permissible level P_{err} , and the actual accuracy of the synchronization infrastructure according to Equation (15). The derived dependencies allow synchronization to be considered as a separate design parameter of a multisensor architecture, on par with the choice of fusion algorithm, when the contribution of synchronization is dominant in the total error.

References

1. Ciuonzo D., Salvo Rossi P., Varshney P. K. Distributed detection in wireless sensor networks under multiplicative fading via generalized score tests. IEEE Internet of Things Journal. 2021. Vol. 8, № 11. P. 9059–9071. https://doi.org/10.1109/JIOT.2021.3056325

2. Varshney P. K. Distributed Detection and Data Fusion. New York: Springer, 1997. https://doi.org/10.1007/978-1-4612-1904-0

3. Banavar M. K., Smith A. D., Tepedelenlioğlu C., Spanias A. Distributed detection over fading MACs with multiple antennas at the fusion center. In: 2010 IEEE International Conference on Acoustics, Speech and Signal Processing (ICASSP). Dallas, TX, USA, 2010. https://doi.org/10.1109/ICASSP.2010.5496170

4. Chen B., Tong L., Varshney P. K. Channel-aware distributed detection in wireless sensor networks. IEEE Signal Processing Magazine. 2006. Vol. 23, № 4. P. 16–26. https://doi.org/10.1109/MSP.2006.1657814

5. Aldalahmeh S. A., Al-Jazzar S. O., McLernon D., Zaidi S. A. R., Ghogho M. Fusion rules for distributed detection in clustered wireless sensor networks with imperfect channels. IEEE Transactions on Signal and Information Processing over Networks. 2019. Vol. 5, № 3. P. 585–597. https://doi.org/10.1109/TSIPN.2019.2901198

6. Cover T. M., Thomas J. A. Elements of Information Theory. 2nd ed. Hoboken: Wiley-Interscience, 2006. 784 p. https://doi.org/10.1002/047174882X

7. Kopetz H., Bauer G. The time-triggered architecture. Proceedings of the IEEE. 2003. Vol. 91, № 1. P. 112–126. https://doi.org/10.1109/JPROC.2002.805821

8. Schmid T., Charbiwala Z., Friedman J., Cho Y. H., Srivastava M. B. Exploiting manufacturing variations for compensating environment-induced clock drift in time synchronization. ACM SIGMETRICS Performance Evaluation Review. 2008. Vol. 36, № 1. P. 97–108. https://doi.org/10.1145/1384529.1375469

9. IEEE Standard for a Precision Clock Synchronization Protocol for Networked Measurement and Control Systems. IEEE Std 1588-2019. New York: IEEE, 2020. https://doi.org/10.1109/IEEESTD.2020.9120376

10. Moreira P., Serrano J., Wlostowski T., Loschmidt P., Gaderer G. White Rabbit: Sub-nanosecond timing distribution over Ethernet. In: 2009 International Symposium on Precision Clock Synchronization for Measurement, Control and Communication. Brescia, Italy, 2009. P. 1–5. https://doi.org/10.1109/ISPCS.2009.5340196

11. Novick A., Lombardi M. Establishing traceability with a GPS disciplined oscillator/clock (GPSDO/GPSDC): A preliminary report. International Foundation for Telemetering ITC International Telemetering Conference. Glendale, AZ, USA, 2022.

12. Mills D. L. Internet time synchronization: The Network Time Protocol. IEEE Transactions on Communications. 1991. Vol. 39, № 10. P. 1482–1493. https://doi.org/10.1109/26.103043

13. Skokowski P., Malon K., Łopatka J. Building the electromagnetic situation awareness in MANET cognitive radio networks for urban areas. Sensors. 2022. Vol. 22, № 3. P. 716. https://doi.org/10.3390/s22030716

14. Mazuro M., Skokowski P., Kelner J. M. Coordinated radio emitter detection process using a group of unmanned aerial vehicles. Sensors. 2025. Vol. 25, № 23. P. 7298. https://doi.org/10.3390/s25237298

15. ITU-R. Next generation spectrum monitoring – proactive, autonomous and data-driven. Report ITU-R SM.2542-0. Geneva: International Telecommunication Union, 2024.

16. Aksu M., Candell R. Requirements for Spectrum Monitoring in Industrial Environments. NIST Interagency/Internal Report 8195. Gaithersburg: National Institute of Standards and Technology, 2017. https://doi.org/10.6028/NIST.IR.8195